Journal of Inflammation Research

Dovepress
open access to scientific and medical research

Open Access Full Text Article

ORIGINAL RESEARCH

RETRACTED ARTICLE: Cardiomyocyte Stim1 Deficiency Exacerbates Doxorubicin Cardiotoxicity by Magnification of Endoplasmic Reticulum Stress

Jiang Zhu[1,*]
Xia Zhang[2,*]
Hong Xie[1]
Yuye Wang[1]
Xiaoxiao Zhang[1]
Zhaoheng Lin[3]

[1]Department of Anesthesiology, The Second Affiliated Hospital of Soochow University, Suzhou, 215008, Jiangsu, People's Republic of China; [2]Department of Anesthesiology, Wuzhong People's Hospital, Suzhou, Jiangsu, 215128, People's Republic of China; [3]Intensive Care Unit, People's Hospital of Xishuangbanna Dai Nationality Autonomous Prefecture, Jinghong City, 666100, Yunnan, People's Republic of China

*These authors contributed equally to this work

Introduction: Doxorubicin (Dox) is an effective anticancer agent, however, its cardiotoxicity remains a challenge. Dysfunction of intracellular calcium ion (Ca^{2+}) is implicated in the process of Dox-induced cardiomyocyte apoptosis although store-operated Ca^{2+} entry (SOCE) is suggested to be responsible for Ca^{2+} entry in cardiomyocytes, the direct role of store-operated Ca^{2+} channels in Dox-related cardiomyocyte apoptosis is unknown.

Materials and Methods: Cardiomyocyte Stim1-specific knockout or overexpression mice were treated with Dox. Cardiomyocytes were pretreated with Stim1 adenovirus or siRNA followed by Dox incubation in vitro. Cardiac function and underlying mechanisms echocardiography were assessed via immunofluorescence, flow cytometry, real-time PCR, Western blotting and immunoprecipitation.

Results: We observed the inhibition of Stim1 expression, association of Stim1 to Orai1 or Trpc1, and SOCE by Dox in mouse myocardium and cardiomyocytes. Orai1 and Trpc1 expression remained unchanged. Cardiomyocyte-specific deficiency of Stim1 exacerbated Dox-induced cardiac dysfunction and myocardial apoptosis. However, specific overexpression of Stim1 in the myocardium was associated with amelioration of cardiac dysfunction and cardial apoptosis. In vitro, STIM1 knockdown potentiated Dox-induced AC16 human cardiomyocyte apoptosis. This apoptosis was attenuated by STIM1 upregulation. Moreover, STIM1 downregulation enhanced Dox-induced endoplasmic reticulum (ER) stress in cardiomyocytes. In contrast, STIM1 overexpression inhibited the activation of the above molecular markers of ER stress. Immunoprecipitation assay showed that STIM1 interacted with GRP78 in cardiomyocytes. This interaction was attenuated in response to Dox treatment.

Conclusion: Our data demonstrate that cardiomyocyte STIM1 binding to GRP78 ameliorates Dox cardiotoxicity by inhibiting pro-apoptotic ER stress.

Keywords: doxorubicin, cardiotoxicity, cardiomyocyte apoptosis, STIM1, endoplasmic reticulum stress

Introduction

Doxorubicin (Dox) is widely used for the treatment of haematologic malignancies and solid tumor, such as leukemia, breast cancer, colorectal cancer, and ovarian cancer.[1,2] Although Dox is an effective anti-tumor therapeutic agent, it causes cumulative cardiotoxicity, encompassing abnormal changes in myocardial structure and function, cardiomyopathy, and even heart failure that may lead to cardiac transplantation or death.[2–5] Cardiomyocyte apoptosis or other forms of cardiomyocyte death, resulting in functional cardiomyocyte loss and irreversible heart injury,

Correspondence: Zhaoheng Lin
Intensive Care Unit, People's Hospital of Xishuangbanna Dai Nationality Autonomous Prefecture, Galan South Road, Jinghong City, 666100, Yunnan, People's Republic of China
Tel +86691-2123836
Fax +8615198406999
Email linzh_med@163.com

Received: 29 January 2021
Accepted: 8 June 2021
Published: 14 August 2021

are considered the major features of Dox-induced cardiotoxicity.[3,6] Importantly, cardiomyocytes are terminally differentiated cells that typically cannot be replicated.[2] Therefore, prevention of cardiomyocyte apoptosis or death may be an effective way to ameliorate Dox cardiotoxicity.

The endoplasmic reticulum (ER) is an important organelle for maintaining biological process and cellular function.[7,8] Excessive accumulation of unfolded and incompletely folded proteins in the ER that exceed the capacity of the protein folding machinery can trigger the unfolded protein response (UPR) and ER stress.[8,9] Recent evidence showed that activation of ER stress contributes to the pathogenesis of cardiovascular diseases, including Dox cardiotoxicity.[10–12] Sustained ER stress can induce cardiomyocytes apoptosis.[9,13] Several UPR signaling sensors have been identified, including protein kinase R-like ER kinase (PERK)/eukaryotic translation initiation factor-alpha (eiF2α)/ATF4/C/EBP-homologous protein (CHOP), inositol-requiring enzyme 1α (IRE1α)/c-Jun N-terminal kinase (JNK), transcriptional factor ATF6, and caspase 12.[14–16] Upon UPR stress, 78 kDa glucose-regulated protein (GRP78) functions as a master regulator by binding to and inactivating the sensors.[17] In the early phase of ER stress, the increased association of GRP78 and unfolded protein substrates releases the sensors to initiate UPR signaling.[9,18]

Disruption of calcium ion (Ca^{2+}) homeostasis is proposed as one of the underlying mechanisms that initiates cell apoptosis and death.[13,19] In addition to non-excitable cells, emerging evidence has demonstrated that store-operated Ca^{2+} entry (SOCE) is also responsible for Ca^{2+} entry in certain excitable cells, including cardiomyocytes.[19–21] Stromal interaction molecule 1 (STIM1), calcium release-activated calcium modulator 1 (CRACM1, also known as ORAI1), and transient receptor potential cation channel subfamily C member 1 (TRPC1) are considered to be the molecular components of store-operated Ca^{2+} channels (SOCCs).[22,23] STIM1, which is located in the ER membrane, serves as a sensor of ER Ca^{2+} level and mediates SOCE.[23] Depletion of ER Ca^{2+} store causes STIM1 oligomerization and its interaction with plasma membrane channels ORAI1 and TRPC1, triggering SOCE.[22]

Although SOCE has been implicated in various pathological conditions of cardiovascular diseases,[19,24,25] there is still no evidence of the direct role of SOCCs in Dox cardiotoxicity. This study aimed to investigate the effects of SOCCs on Dox cardiotoxicity and cardiomyocyte apoptosis. The results suggest that cardiomyocyte STIM1 may be a potential therapeutic target for the treatment of Dox cardiotoxicity.

Methods

Materials and Reagents

Antibodies against STIM1, STIM2, ORAI1, and TRPC1 were obtained from Alomone (Jerusalem, Israel). Bcl-2, Bax, GRP78, caspase 12, β-actin, flag tag, and myc tag antibodies were purchased from Cell Signaling Technology (Danvers, MA). Antibodies to α-actinin, CHOP, ATF4, ATF6, p-eiF2α, eiF2α, p-PERK, PERK, p-JNK, and JNK were from Santa Cruz Biotechnology Inc. (Santa Cruz, CA). Adenovirus carrying human STIM1 (Ad-STIM1), negative control Lacz adenovirus (Ad-Lacz), STIM1 siRNA, and non-specific siRNA oligonucleotides (negative siRNA) were synthesized from RiboBio Co., Ltd (Guangzhou, China). Mammalian expression plasmids for myc-tagged GRP78 and flag-tagged STIM1 were constructed by BioVector NTCC Inc. (Beijing, China). Dulbecco's minimal essential medium (DMEM), OptiMEM I medium, fetal bovine serum (FBS), penicillin, streptomycin, and Lipofectamine 2000 were obtained from Invitrogen (Carlsbad, CA). All other reagents were purchased from Sigma Chemical Co. (St. Louis, MO) unless otherwise specified.

Cardiomyocyte-Specific Stim1 Knockout Mouse

All animal experiments were approved by the Institutional Animal Care and Use Committee of Soochow University (Suzhou, Jiangsu) and conformed to the "Guide for the Care and Use of Laboratory Animals" of the National Institute of Health in China. Mice were received standard chow and water, and maintained on an alternating 12-h light-dark cycle. Stim1 flox/flox ($Stim1^{f/f}$; B6 (Cg)-*Stim1*^{tm1Rao}/J; stock no. 023350) mice and MHC-cre mice (B6.FVB-Tg (*Myh6-cre*)^{2182Mds}/J; stock no. 011038) were obtained from Jackson Laboratory (Bar Harbor, ME). Mice were backcrossed to a C57BL/6J genetic background for at least nine generations. Cardiomyocyte-specific Stim1 knockout mice ($Stim1^{CKO}$) were generated by mating $Stim1^{f/f}$ with MHC-cre mice, in which exon 2 of Stim1 was flanked by two flox sites. At 4 weeks of age, genomic DNA was extracted from the tail snips. Genotypes were confirmed with the primers to

Cre and Stim1 flox alleles. $Stim1^{f/f}$ mice were used as control animals unless stated otherwise.

Animal Model and Adenovirus Delivery

Wild type (WT) C57/BL6 mice were purchased from the Jackson Laboratory. A Dox-induced cardiotoxicity mouse model was established as described previously.[2] Briefly, 5–6-week-old male $Stim1^{f/f}$ mice, $Stim1^{CKO}$ mice, or WT mice were anesthetized and implanted with a mini osmotic pump (model 2002; Alzet, Palo Alto, CA) containing 200 µL of either saline (vehicle) or Dox at a dose of 15 mg/kg of body weight, at a rate of 0.5 µL/h, for a period of 14 days. For survival rate measurement, these mice were monitored until day 40. For the delivery of AAV (serotype 9) encoding mouse Stim1 (Oobi, Shanghai, China) or Lacz in WT mice, AAV-Stim1 (2×10^{11} plaque forming units [pfu]/mouse) or AAV-Lacz (2×10^{11} pfu/mouse) was injected into the left ventricular (LV) cavity through the tip of the heart with a 32-gauge needle (approximately 10 different sites), followed by intraperitoneal anesthetization with pentobarbital sodium (50 mg/kg) 3 days before Dox administration.

Cell Culture and Treatment

AC16 cardiomyocytes were purchased from the Cell Bank of Chinese Academy Medical Science (Shanghai, China). The cells were cultured in DMEM containing 10% FBS and 1% penicillin–streptomycin solution (100× all from Gibco, Carlsbad, CA) in an incubator containing 5% CO_2 at 37°C. Ad-STIM1 was added to upregulate STIM1 expression in cultured cells for 24 h before Dox treatment (1 µmol/L) for another 24 h. Ad-Lacz was used as a negative control. For siRNA or plasmid transfection, STIM1 siRNA, negative siRNA, or plasmids were diluted with OptiMEM I medium and transfected into cells with Lipofectamine 2000 following the manufacturer's instructions. The siRNA sequence targeting STIM1 was 5′-GGCTC GGA ACA CTC-3′.

Western Blotting and Immunoprecipitation

Protein was extracted from cardiomyocytes or from the anterior wall of LV in ice-cold lysis buffer (50 mmol/L Tris, 150 mmol/L NaCl, 1 mmol/L EDTA, 1 mmol/L phenylmethylsulfonyl fluoride, 2 mmol/L $Na_4P_2O_7$, 1 mmol/L sodium fluoride, 1 mmol/L Na_3VO_4, and 0.25% sodium deoxycholate, 1% Triton X-100, pH 7.5) containing a protease inhibitor (Beyotime, Shanghai). The protein concentrations were quantified using the BCA Protein Assay Kit (Pierce, Rockford, IL). Equal concentrations of protein were separated by sodium dodecyl sulfate-polyacrylamide gel electrophoresis and then transferred to polyvinylidene fluoride membranes (Bio-Rad Laboratories, Hercules, CA). The membranes were blocked in 5% non-fat dried milk in Tris-buffered saline (TBS) for 1 h, followed by incubation with appropriate primary antibodies overnight at 4°C. Afterwards, the membranes were incubated with horseradish peroxidase-conjugated anti-mouse or anti-rabbit secondary antibodies (Cell Signaling Technology) at room temperature for 1 h. After washing with TBS containing Tween three times for 10 min each time, the antigen-antibody complex was detected using ECL chemiluminescence reagent (Thermo Scientific, Waltham, MA). Quantification of all immunoblots was performed using IMAGE software (Version 1.41; NIH, Bethesda, MD, USA). For immunoprecipitation, protein lysates were co-incubated with A/G agarose beads (Santa Cruz Biotechnology Inc.) and anti-STIM1, anti-GRP78, or anti-myc tag antibody at 4°C overnight. The amount of bound proteins in the immunoprecipitated protein was determined using the indicated antibodies.

qPCR

Total RNA were isolated from LV using the RNAeasy Kit (Qiagen, Venlo, Netherlands). qPCR was performed with a Fast SYBR Green Master Mix Kit (Applied Biosystems) to determine the mRNA expression of Stim1. The levels of mRNA were quantified with the $2^{(-\Delta\Delta ct)}$ and normalized to GAPDH. The primer sequences for qPCR are as follows: Stim1, forward 5′-ggccacaggcttaaaacagac-3′, reverse 5′-cagtctacagcctagcaccc-3′; GAPDH, forward 5′-cttcacca ccatggagaaggc-3′, reverse 5′-ggcatggactgtggtcatgag-3′.

Intracellular Ca^{2+} Concentration $[Ca^{2+}]_i$ Measurements

Cardiomyocytes were seeded in 25-mm coverslips after incubation with Dox for 24 h. The cells were loaded with Fura 2-AM (2 µmol/L) in Krebs solution (in mmol/L: 119 NaCl, 2.5 KCl, 1 NaH_2PO_4, 1.3 $MgCl_2$, 20 HEPES, 11 glucose, 0.5 EGTA, pH 7.4) for 30 min at 37°C. Tg (1 µmol/L) was used to deplete Ca^{2+} stores followed by the addition of 1.8 µmol/L of Ca^{2+}. $[Ca^{2+}]_i$ was analyzed with Cell^R software when examined using a model IX81 wide-field inverted microscope (Olympus, Tokyo, Japan) at wavelengths of 340 nm and 380 nm. The average

fluorescence was calculated by counting 10 random fields (20 cells in each field) per group in six independent experiments.

Electrophysiology

Whole cell currents were recorded using an Axopatch 200B patch clamp amplifier (Axon Instruments, Foster City, CA). Cells were seeded in coverslips and perfused with an external Ringer's solution (in mmol/L: 145 NaCl, 5 CsCl, 1 $MgCl_2$, 1.3, 1 $CaCl_2$, 10 Hepes, 10 glucose, pH 7.3). The patch pipette had resistances between 3 and 5 MΩ after filling with standard intracellular pipette solution that contained the following (in mmol/L): 8 NaCl, 10 Hepes, 10 EGTA, and 150 cesium methane, pH 7.2. Cells were held at a potential of −60 mV and voltage ramps ranged from −100 to +100 mV (50 ms duration). Currents were recorded at 2 kHz and sampled at 5 kHz, and analyzed using pCLAMP 10.0 software (Axon Instruments).

TUNEL Staining

Cardiomyocyte apoptosis was measured by the TUNEL assay using an In Situ Cell Death Detection kit (Roche, Mannheim, Germany). The frozen sections were incubated with primary antibody against α-actinin overnight at 4°C followed by incubation with Cy3-labeled secondary antibody (Invitrogen) for 1 h at room temperature. The sections were incubated with TUNEL reaction mixture for 1 h at 37°C in the dark. 4′,6-Diamidino-2-phenylindole (DAPI) staining was performed for total nuclei quantification. Images were observed and captured using a model LSM710 confocal microscope (Zeiss Microsystems, Mannheim, Germany). The percentage of TUNEL-positive cells (green fluorescence) in the total cells of the cross-sectional area was used to quantify cardiomyocyte apoptosis using ImageJ software (NIH).

Echocardiography

Cardiac function was assessed in conscious mice by echocardiographic analysis using a high-resolution ultrasound imaging system (Vevo770; Visual Sonics, Toronto, ON, Canada). Before the evaluation, conscious mice were trained for echocardiographic measurements over a period of 3 days using the method described previously.[26] LV posterior wall thickness (LVPWth), LV end-diastolic diameter (LVDd), LV end-systolic diameters (LVDs), LV ejection fraction (EF), and LV fractional shortening (FS) were calculated.

Cell Apoptosis Assay by Annexin V/PI Staining

Cardiomyocyte apoptosis was measured using the FITC Annexin V Apoptosis Detection Kit (KeyGEN Biotech, Nanjing, China) according to the manufacturer's instructions. Cultured cells were washed with phosphate buffer saline twice and resuspended in a binding buffer containing FITC-conjugated Annexin V and propidium iodide for 15 min in the dark at room temperature. The stained apoptotic cells were analyzed by flow cytometry (Accuri C6; BD Biosciences, San Diego, CA) and calculated following the manufacturer's protocol (BD Biosciences).

Cell Viability Assay

Cell viability was determined by cell counting kit-8 (CCK-8; Yiyuan Biotechnology, Guangzhou, China) according to the manufacturer's protocols. After corresponding treatment, 10 μL of CCK8 was added to each well for an additional 3 h at 37°C. The absorbance of each well was measured with a SPECTRA MAX190 spectrophotometer (Molecular Devices, Sunnyvale, CA) at a wavelength of 450 nm.

Biochemical Assay

Blood samples were harvested and centrifuged for 10 min at 3000 × g to obtain serum. LDH level in serum and cell culture medium was determined using the CytoTox 96 Non-Radioactive Cytotoxicity Assay kit (Promega, Madison, WI). The level of cTnT in serum was measured using an ELISA kit (MLBIO Biotechnology, Co., Ltd., Shanghai, China). All assays were performed according to the manufacturer's instructions.

Immunofluorescent Staining

To observe the co-localization of STIM1 and GRP78 in cardiomyocytes, cells were fixed and labeled with mouse-anti-STIM1 (Novus Biologicals, CO) and rabbit-anti-GRP78 antibodies. Samples were then washed three times with PBS for 3 min and then were incubated with appropriate secondary antibodies (anti-mouse FITC antibody for labeling STIM1 and anti-rabbit Cy3 antibody for labeling GRP78, Jackson ImmunoResearch, PA) for 1 h at room temperature. Fluorescent images were acquired using the Zeiss Axioplan 2 fluorescence microscopy.

Statistical Analyses

All data are expressed as mean value ± standard error of the mean (SEM). Statistical analysis was performed using

SPSS 18.0 software (SPSS Inc., Chicago, IL) using an unpaired two-tailed Student's *t*-test or one-way ANOVA, followed by the Bonferroni multiple-comparison test. P<0.05 was considered statistically significant.

Results

Decreased Stim1 Expression in Myocardium in Response to Cardiotoxicity

To determine the function of SOCCs in cardiotoxicity, we initially examined whether the expression of SOCCs was altered in the myocardium in response to Dox treatment. Although the expression of Orai1 and Trpc1 was unchanged in the myocardium of mice treated with Dox for 14 days, a marked decrease in Stim1 expression was observed in Dox-treated mice when compared with vehicle-treated mice (Figures 1A and S1A). Interestingly, Dox administration did not alter the mRNA levels of Stim1 in the myocardium, suggesting the involvement of post-translational regulation by Dox (Figure S1B). In addition, when cardiomyocytes were treated with Dox for different time periods, STIM1 protein expression was gradually decreased by Dox. This finding further supported the in vivo results (Figure 1B). STIM1 is a key Ca^{2+} movement regulator that interacts with ORAI1 and TRPC1 upon store depletion to initiate Ca^{2+} entry via SOCE.[22,23] Therefore, we investigated the functional interaction between Stim1 and Orai1 or Trpc1. Immunoprecipitation results showed that Dox treatment led to a sharp decrease in the binding of Stim1 to Orai1 and Trpc1 in myocardial tissues (Figure 1C and D). Given the importance of STIM1 expressi[illegible]its interaction with ORAI1 or TRPC1, we next in[illegible]stigated wh[illegible]her SOCE was altered by Dox in cardiomyoc[illegible]s. In the ab[illegible]nce of extracellular Ca^{2+}, the thapsi[illegible]rgin (Tg)-[illegible]duced [illegible]crease in store Ca^{2+} release (first [illegible]eak) wa[illegible]inhibite[illegible]y Dox treatment. Furthermore, SOCE [illegible]du[illegible]ed by the addition of 2 mmol/L extracellular Ca^{2+} was [illegible]lso in[illegible]bited by Dox treatment (Figure 1[illegible] an[illegible]F). Importa[illegible], Dox treatment significantly decreased store-o[illegible]rated Ca^{2+} currents in cardiomyocytes ([illegible]gure 1G and H). [illegible]aken together, these results indicate [illegible]at Dox inhi[illegible]its Ca^{2+} release and SOCE, at least in part by

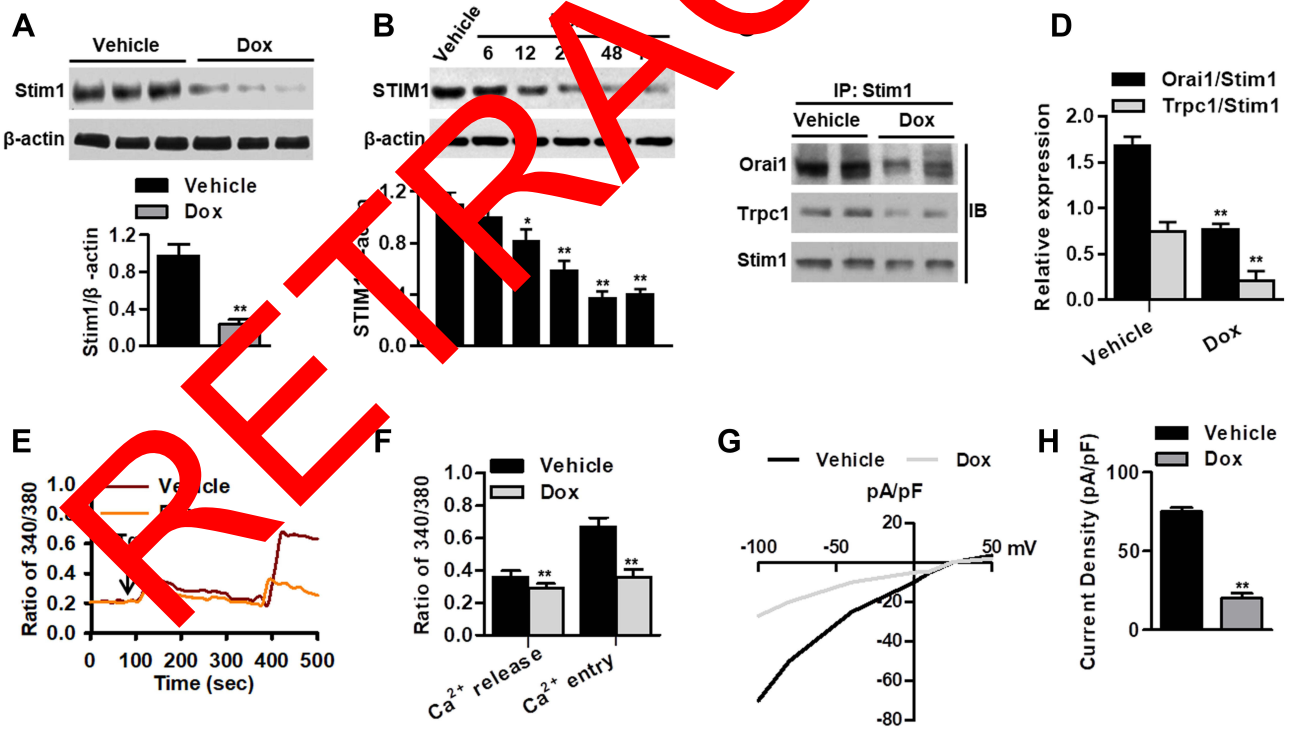

Figure 1 Dox treatment reduces Stim1 expression and SOCE in cardiomyocytes. (**A**) Western blotting analysis of Stim1 expression in myocardium of mice after vehicle or Dox treatment for 14 days. **P<0.01 vs vehicle, n=12/group. (**B**) Cardiomyocytes were treated with Dox (1 μmol/L) for different times as indicated. The expression of STIM1 was determined by Western blotting. *P<0.05, **P<0.01 vs vehicle, n=6. (**C**) Immunoblotting (IB) for Orai1 or Trpc1 after immunoprecipitation (IP) with anti-Stim1 antibody in myocardium from vehicle- or Dox-treated mice. (**D**) Densitometric analysis for the amount of Orai1 or Trpc1 in immunoprecipitated Stim1 protein. **P<0.01 vs vehicle, n=5/group. (**E**) Cardiomyocytes were loaded with Fura 2-AM probe and subjected to Ca^{2+} imaging experiments. (**F**) Quantification of fluorescence ratio (340/380) representing the thapsigargin (Tg)-induced Ca^{2+} store release and SOCE in cardiomyocytes. **P<0.01 vs vehicle, n=20. (**G**) Dox treatment decreased store-operated Ca^{2+} currents in cardiomyocytes. Average IV curves under vehicle and Dox conditions were shown. (**H**) Average current intensity was calculated. **P<0.01 vs vehicle, n=15.

decreasing STIM1 expression and its interaction with ORAI1 or TRPC1.

Cardiomyocyte-Specific Deficiency of Stim1 Exacerbates Dox-Induced Myocardial Injury

We next investigated whether the alteration of Stim1 in response to Dox is involved in Dox-induced cardiotoxicity. Cardiomyocyte-specific knockout mice were administrated Dox for 14 days (Figure S2A). Stim1 deficiency did not affect the expression of other isoforms of the Stim family (Figure S2B), excluding possible compensatory effects. As expected, Dox administration significantly increased the serum levels of lactate dehydrogenase (LDH) and cardiac troponin T (cTnT), which are the two well-established makers of cardiac injury. Loss of Stim1 in cardiomyocytes further increased the levels of LDH and cTnT (Figure 2A and B). In addition, Dox-induced mortality was significantly higher in Stim1^{CKO} mice than in their control littermates (Figure 2C). Echocardiography examination showed that Stim1 knockout further promoted the Dox-induced changes in the morphology of the left ventricular, as evidenced by decreased LVPWth and increased LVDd and LVDs (Figure 2D and Table 1). Dox administration also markedly impaired cardiac functions in mice, as indicated by decreased EF and fractional shortening FS values. The impairment of cardiac function was more pronounced in Stim1^{CKO} mice than in Stim$^{f/f}$ mice (Table 1). The body weight and food intake were lower and the ratio of lung to body weight was higher in Dox-treated mice than in vehicle-treated mice. However, these alterations did not differ between Dox-treated Stim$^{f/f}$ mice and Stim1^{CKO} mice. Moreover, LV/body weight ratio was similar among th[illegible]ups (Table S1).

Upregulation of Stim1 in Myocard[illegible]um Ameliorates Cardi[illegible]toxicity

We subsequently ove[illegible]presse[illegible] of Stim1 in the myocardium to confirm t[illegible] role [illegible]tim1 in [illegible]ox cardiotoxicity. Western blottin[illegible] results con[illegible]med that the expression of Stim1 was [illegible]ucce[illegible]fully eleva[illegible]ed in the myocardium after in[illegible]ection with [illegible]deno-associated virus (AAV)-Stim[illegible] (Figure S3). In co[illegible]trast to what was observed in Sti[illegible]^{CKO} mice, AAV-Stim1-infected mice treated with Dox[illegible]howed re[illegible]uced serum LDH and cTnT levels

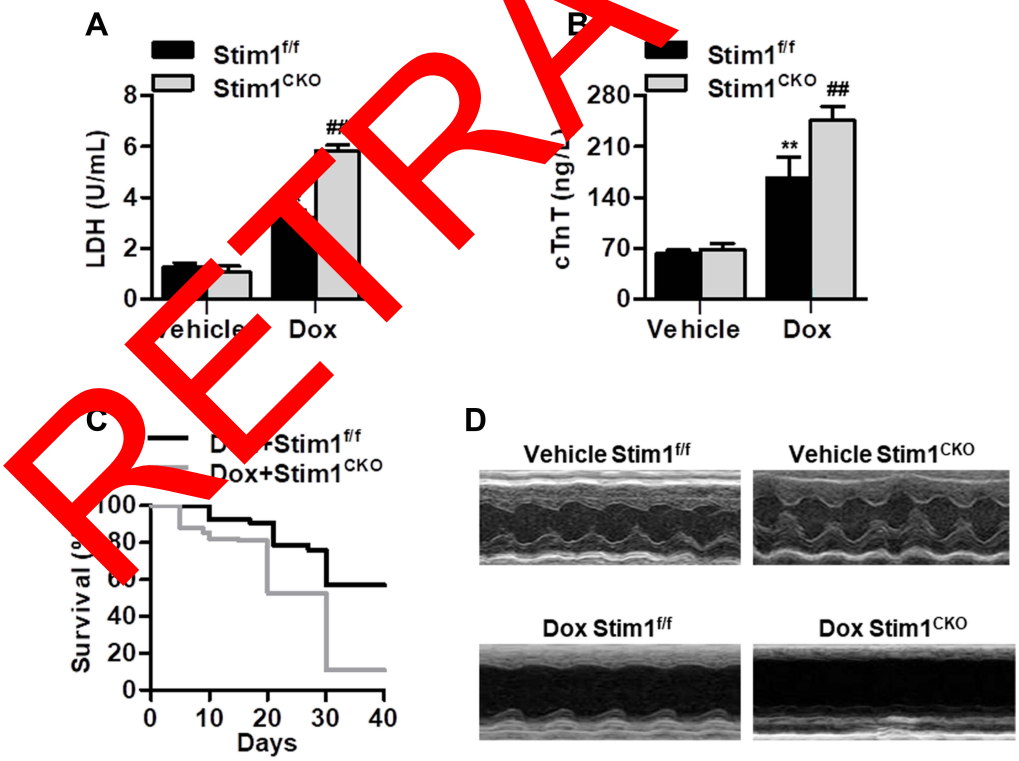

Figure 2 Cardiomyocyte Stim1 deficiency enhances Dox-induced myocardial injury. (**A** and **B**) Cardiomyocyte-specific Stim1 knockout mice (Stim1^{CKO}) and their control littermates (Stim1$^{f/f}$) were treated with Dox (15 mg/kg body weight) for 14 days. LDH (**A**) and cTnT (**B**) release in serum were measured by a commercial kit. n=12/group. **P<0.01 vs vehicle+Stim1$^{f/f}$; ##P<0.01 vs Dox+Stim1$^{f/f}$. (**C**) Survival curves were recorded until day 40 after the start of Dox treatment. n=20/group. (**D**) Echocardiography was performed as described in the Methods section. Representative M-mode echocardiography from the four groups of mice with different treatments. n=12/group.

Table 1 Echocardiographic Characteristics of Left Ventricular Parameters in Mice with Different Treatments

Characteristics	Vehicle		Doxorubicin		Vehicle		Doxorubicin	
	Stim1$^{f/f}$	Stim1^{CKO}	Stim1$^{f/f}$	Stim1^{CKO}	AAV-Lacz	AAV-Stim1	AAV-Lacz	AAV-Stim1
LVPWth (mm)	1.81±0.14	1.76±0.15	1.44±0.13**	1.09±0.11$^{\#\#}$	1.77±0.13	1.83±0.15	1.33±0.09**	1.58±0.13$^{\#\#}$
LVDd (mm)	6.13±0.33	6.21±0.42	7.55±0.36**	8.47±0.31$^{\#\#}$	6.09±0.43	6.19±0.38	7.70±0.35**	6.54±0.22$^{\#\#}$
LVDs (mm)	2.45±0.14	2.54±0.22	3.23±0.23**	3.99±0.41$^{\#\#}$	2.56±0.18	2.68±0.23	3.32±0.31**	2.77±0.17$^{\#\#}$
EF%	68.24±5.56	68.25±6.25	51.20±4.55**	38.15±4.67$^{\#\#}$	65.15±6.15	67.15±4.01	48.45±5.15**	59.15±5.09$^{\#\#}$
FS%	54.50±5.45	56.45±6.95	36.45±4.98**	24.14±3.60$^{\#\#}$	56.15±5.11	58.14±7.14	38.45±5.01**	49.14±4.98$^{\#\#}$

Notes: Data are expressed as mean ± SEM. **P<0.01 vs vehicle+Stim1$^{f/f}$ or vehicle+AAV-Lacz; $^{\#\#}$P<0.01 vs Dox+Stim1$^{f/f}$ or Dox+AAV-Lacz, n=12/group.
Abbreviations: LVPWth, left ventricular end-diastolic posterior wall thickness; LVDd, left ventricular end-diastolic diameter; LVDs, left ventricular end-systolic diameter; EF, ejection fraction of left ventricle; FS, fractional shortening of left ventricle.

compared with Dox-treated AAV-β-galactosidase (Lacz)-infected mice (Figure 3A and B). Upregulation of Stim1 was associated with lower mortality in response to Dox challenge (Figure 3C). Moreover, Dox-induced decrease in LVPWth and increase in LVDd and LVDs were inhibited in AAV-Stim1-infected mice (Figure 3D and Table 1). Similarly, after Dox treatment, mice overexpressing Stim1 in the myocardium exhibited higher EF and FS percentage compared to control littermates (Table 1).

Stim1 Deficiency Potentiates Dox-Induced Myocardial Apoptosis

Cardiomyocyte apoptosis has been identified as an important contributor to cardiotoxicity.[2,6] We thus examined the effect of Stim1 on cardiomyocyte apoptosis. Terminal deoxynucleotidyl transferase dUTP nick end labeling (TUNEL) staining revealed that the extent of cardiomyocyte apoptosis in the myocardium did not differ between vehicle-treated Stim1^{CKO} and Stim1$^{f/f}$ mice. After Dox treatment, the number of apoptotic cells was significantly

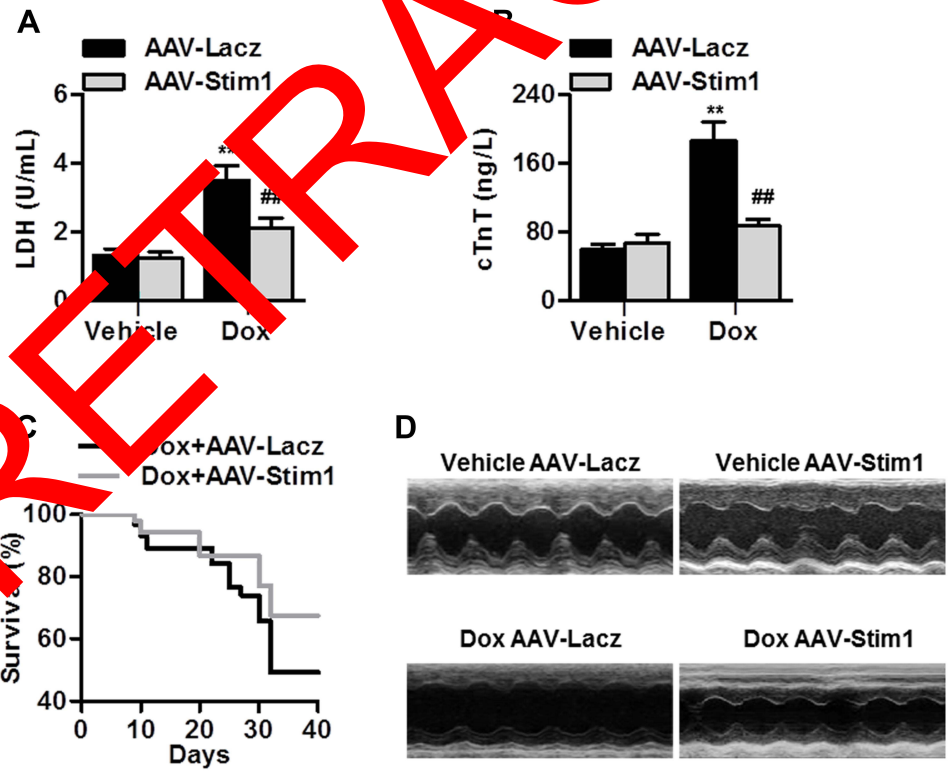

Figure 3 Stim1 overexpression attenuates Dox-induced cardiotoxicity. (**A** and **B**) Mice were infected with AAV-Lacz or AAV-Stim1, and then infused with Dox (15 mg/kg of body weight) with an osmotic pump for 14 days. Serum LDH (**A**) and cTnT (**B**) concentration was examined. n=13/group. **P<0.01 vs vehicle+AAV-Lacz; $^{\#\#}$P<0.01 vs Dox +AAV-Lacz. (**C**) Survival curves were recorded until day 40 after Dox treatment. n=20/group. (**D**) Echocardiographic analysis of heart function and representative photographs were shown. n=12/group.

increased and this increase was further enhanced by cardiomyocyte-specific knockout of Stim1 (Figures 4A and S4A). However, upregulation of Stim1 in the myocardium by infection of AAV-Stim1 markedly inhibited the increase in cardiomyocyte apoptosis (Figures 4B and S4B). In addition, the expression of apoptosis-related molecules was determined. Western blotting showed that the myocardial expression of B-cell lymphoma 2 (Bcl-2) was decreased while the expression of Bcl-2-like protein 4 (Bax) was increased after Dox administration, leading to a decrease in the ratio of Bcl-2 to Bax, which appears to determine the survival or death fate of cell.[27] Lack of cardiomyocyte Stim1 further augmented the effect of Dox on Bcl-2 and Bax expression and the Bcl-2/Bax ratio, whereas Stim1 upregulation counteracted these effects of Dox (Figure 4C–J). The imbalance of Bcl-2 and Bax could lead to mitochondrial membrane potential depolarization, which is followed by cytochrome c release from mitochondrial to cytosol, and combines with caspase-3 cleavage, triggering apoptosis.[2,28,29] After Dox stimulation, the translocation of cytochrome c from mitochondria to cytoplasm and cleaved caspase-3 expression was significantly increased in the myocardium. The increased cytochrome c translocation and cleaved caspase-3 expression were further enhanced in Stim1^{CKO} mice but were inhibited in AAV-Stim1-treated mice (Figure S3A and B).

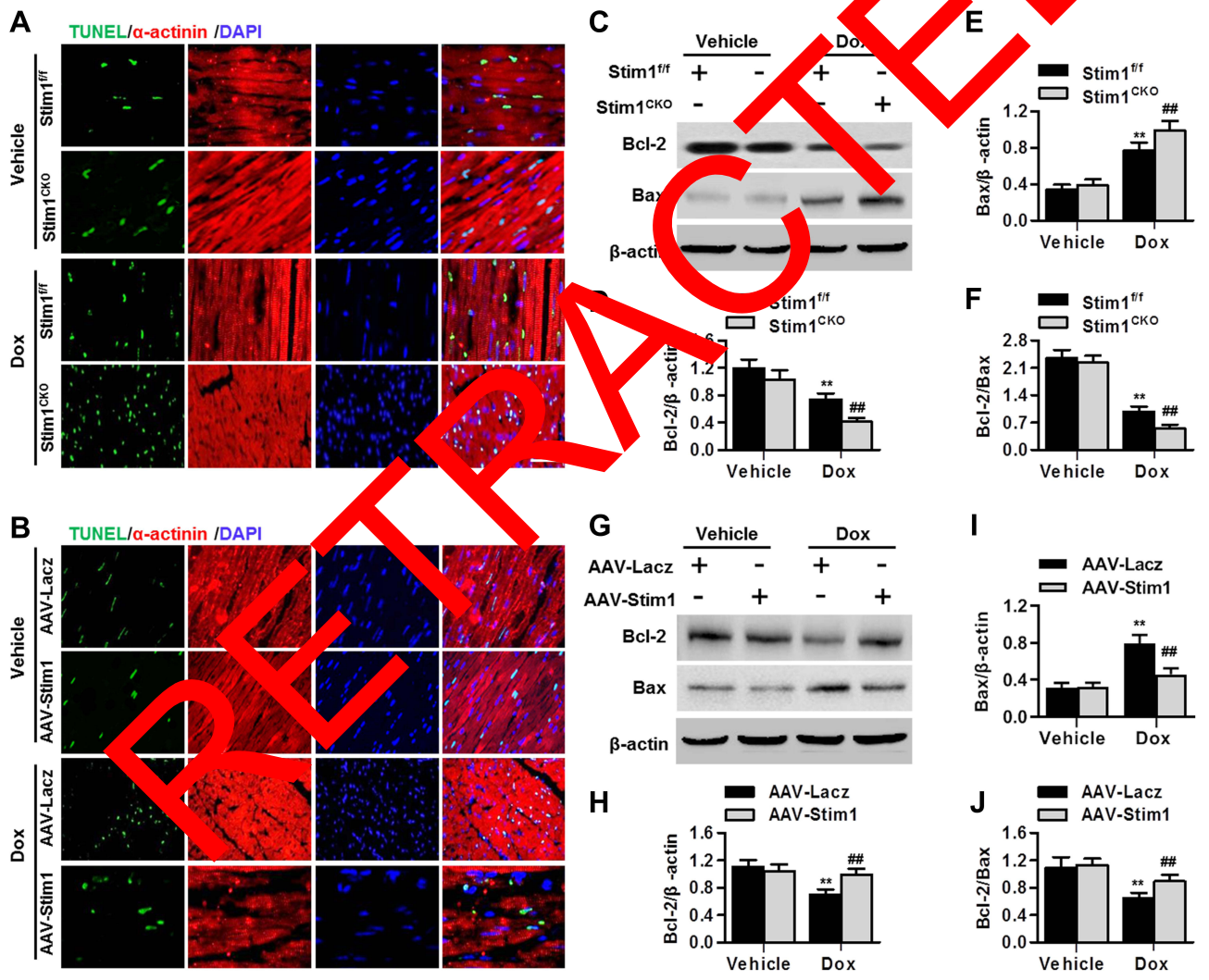

Figure 4 Stim1 knockout exacerbates Dox-induced myocardial apoptosis. (**A** and **B**) Cell apoptosis in the cross-sectional area of myocardium from Stim1^{CKO} mice, Stim1$^{f/f}$ mice (**A**), AAV-Lacz-infected mice and AAV-Stim1-infected mice (**B**) treated with vehicle or Dox was examined by TUNEL staining. Representative TUNEL (green) and α-actinin (red) stained photographs of cardiomyocytes in myocardial tissues. The nuclei was counterstained with DAPI (blue). n=6/group. Scale bar, 50 μm. (**C–J**) The protein expression of Bcl-2 and Bax in myocardium from the above groups were determined. Representative images of Western blotting were shown (**C** and **G**). Densitometric analysis of Bcl-2 (**D** and **H**), Bax (**E** and **I**), and the ratio of Bcl-2 to Bax (**F** and **J**) were performed. **P<0.01 vs vehicle+Stim1$^{f/f}$ or vehicle+AAV-Lacz; ##P<0.01 vs Dox +Stim1$^{f/f}$ or Dox+AAV-Lacz, n=8/group.

These results suggest that Stim1 attenuates Dox cardiotoxicity via inhibiting myocardial apoptosis.

STIM1 Knockdown Promotes Dox-Induced Cardiomyocyte Apoptosis in vitro

To further confirm whether the anti-apoptotic effects of STIM1 were reproducible in vitro under Dox conditions, cardiomyocytes were treated with STIM1 siRNA or adenovirus. As expected, STIM1 small interfering RNA (siRNA) specifically decreased the expression of STIM1, while Ad-STIM1 infection markedly increased STIM1 expression in cardiomyocytes (Figure S6A and B). Consistent with the results of TUNEL staining, the Annexin V-fluorescein isothiocyanate/propidium iodide (FITC/PI) data revealed that Dox insult significantly increased the percentage of apoptotic cells, which was enhanced by STIM1 downregulation but inhibited by STIM1 overexpression (Figure 5A–D). Similarly, upon Dox stimulation, knockdown of STIM1 markedly decreased the viability of cardiomyocyte, whereas upregulation of STIM1 was associated with increased cell viability (Figure 5E and F). Furthermore, the Dox-induced release of LDH in cardiomyocyte was more pronounced in STIM1 siRNA-treated cells than in negative siRNA-treated cells (Figure 5G). However, Stim1 overexpression revealed the opposite effects (Figure 5H).

STIM1 Downregulation Enhances Dox-Induced ER Stress in Cardiomyocytes

Since the shortage of ER Ca^{2+} is critically associated with activation of pro-apoptotic ER stress signaling,[18] the effects of STIM1 on ER stress in cardiomyocytes were evaluated. Similar to previous studies,[6,30,31] Dox could activate the molecular markers of ER stress, such as p-PERK and its downstream pro-apoptotic molecules p-eiF2α, ATF4 and CHOP as well as p-JNK and ATF6, but had no effect on the cleavage of caspase 12 (Figures 6A–H and S7A–F). The findings suggested that Dox markedly induces ER stress in cardiomyocytes. Silencing of STIM1 further enhanced Dox-induced PERK and eiF2α phosphorylation and ATF4 and CHOP expression, while STIM1 overexpression was associated with inhibition of PERK/eiF2α/ATF4/CHOP activation (Figure 6A–H). STIM1 downregulation or upregulation did not alter the activation of JNK and ATF6 (Figure S7A–D). In line with the in vitro results, cardiomyocyte-specific deficiency of Stim1 also markedly enhanced the Dox-induced increase in p-PERK, p-eiF2α, ATF4, and CHOP levels in the myocardium (Figure S8A–D). These data suggest that STIM1 ameliorates cardiomyocyte apoptosis by inhibiting ER stress.

STIM1 Attenuates ER Stress by Binding to GRP78

To understand how STIM1 inhibits ER stress, we investigated whether there is a functional interaction between STIM1 and the upstream molecule of UPR signaling GRP78. Confocal microscopy of cardiomyocytes revealed similar patterns for STIM1 and GRP78, and image superimposition showed marked co-localization of the STIM1 and GRP78 (Figure 7A). In addition, an immunoprecipitation assay clearly showed that STIM1 interacted with GRP78 in cardiomyocytes (Figure 7B). To further validate this interaction, the cells were co-transfected with a flag-tagged STIM1 vector and a myc-tagged GRP78 vector. Immunoprecipitation of GRP78-myc with anti-myc antibody led to co-immunoprecipitation of STIM1-flag exogenously (Figure 7C). Importantly, the interaction between Stim1 and Grp78 was significantly blocked in the myocardium of Dox-treated mice compared with vehicle-treated mice (Figure 7D). Similarly, the in vitro results further supported that this interaction was inhibited in cardiomyocytes by Dox stimulation (Figure 7E). These data indicate that the reduced STIM1 expression and subsequent STIM1/GRP78 interaction may free GRP78 to initiate UPR signaling and ER stress.

Discussion

We observed inhibition of STIM1 expression and SOCE in cardiomyocytes during Dox cardiotoxicity. In addition, to the best of our knowledge, we demonstrate for the first time that cardiomyocyte Stim1 protects against Dox-induced myocardial injury by inhibiting cardiomyocyte apoptosis, while Stim1 cardiomyocyte-specific knockout mice show an opposite phenotype. The pro-apoptotic effects of STIM1 knockdown in cardiomyocytes are associated with ER stress. These findings further emphasize the critical role of SOCCs in maintaining Ca^{2+} homeostasis and cellular function in cardiomyocytes.

Recently, SOCCs have attracted increasing attention concerning the regulation of Ca^{2+} entry in excitable cells, including cardiomyocytes.[13,19,21] The existence of SOCCs

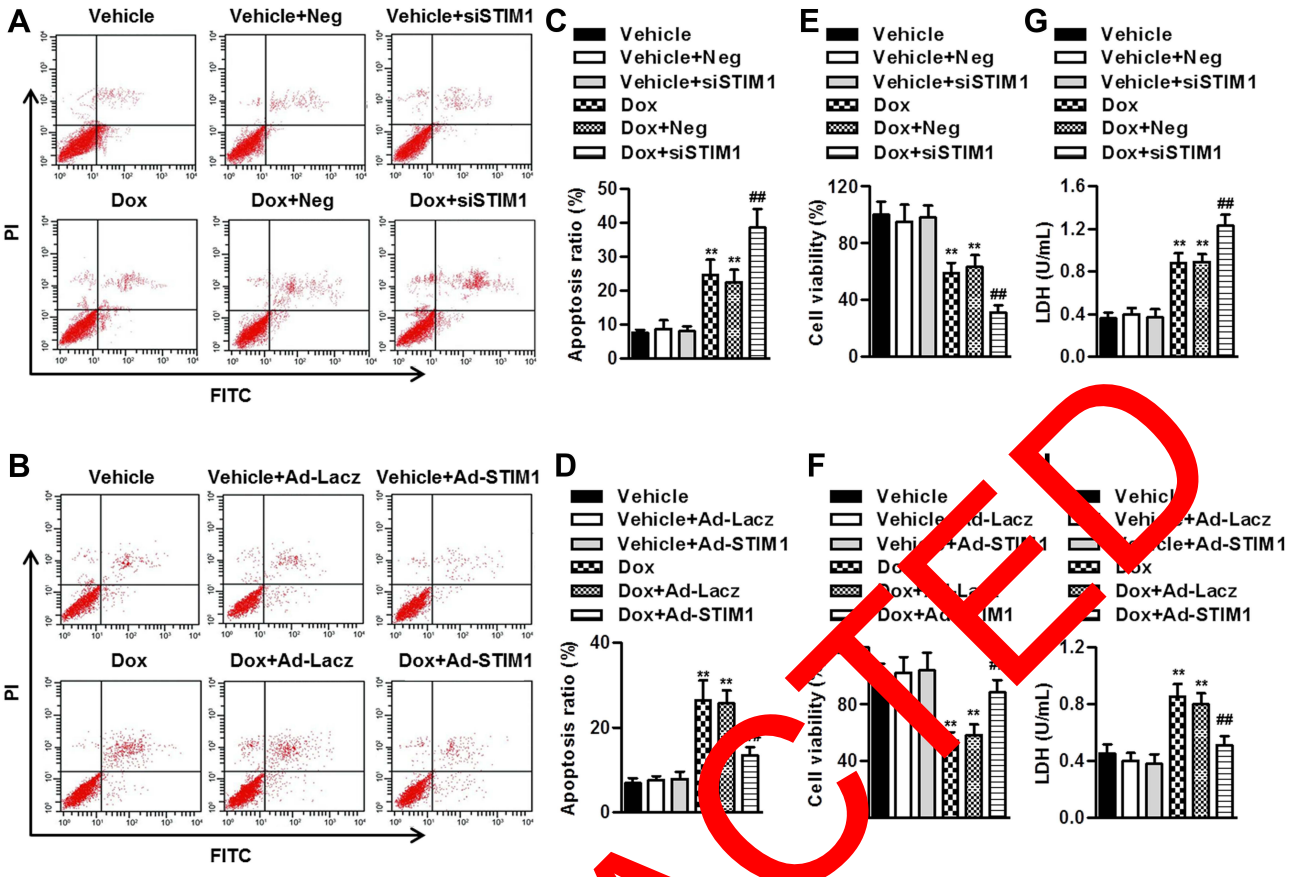

Figure 5 STIM1 deficiency promotes cardiomyocyte apoptosis induced by Dox. (**A**–**D**) Cardiomyocytes were treated with negative siRNA (Neg, 40 nmol/L), STIM1 siRNA (siSTIM1, 40 nmol/L) (**A**), Lacz adenovirus (Ad-Lacz, 40 MOI) or STIM1 adenovirus (Ad-STIM1, 40 MOI) (**B**) for 24 h in prior to Dox (10 μmol/L) incubation for another 24 h. Cell apoptosis was determined by Annexin V/PI staining following flow cytometry (**A** and **B**). Quantitative analysis of the percentage of apoptotic cells (**C** and **D**). (**E** and **F**) After the above-mentioned treatment, cell viability was assessed with CCK-8 assay. (**G** and **H**) At the end of the experiment, cell medium were harvested and LDH release was measured. Data were expressed as mean ± SEM. **P<0.01 vs vehicle, ##P<0.01 vs Dox, n=5–8.

in cardiomyocytes raises the intriguing possibility that SOCCs may be critical for cardiac function.[21,32] Indeed, STIM1-mediated SOCE is necessary for adaptive hypertrophy and protects against heart failure.[3] Although a recent study reported that SOCE was involved in epirubicin cardiotoxicity, its precise role in this process and related mechanisms are still poorly understood.[34] Presently, Dox inhibited SOCE in cardiomyocytes. The Ca^{2+} entry inhibition may be dependent on Stim1 expression downregulation because Dox decreased cardiac Stim1 expression both in vitro and in vivo. Several factors have been suggested to contribute to Dox cardiotoxicity. However, the precise mechanisms and the involvement of Ca^{2+} remain unclear. Consistent with previous studies in several animal models,[2,35,36] a marked impairment of cardiac function in mice was observed after Dox challenge, concomitant with increased mortality. The deleterious effects of Dox were significantly exacerbated in Stim1 cardiomyocyte-specific knockout mice. However, upregulation of Stim1 was effective in improving cardiac function. Cardiomyocyte Stim1 deficiency had no effects on the Dox-induced decrease in body weight and food intake and increase in lung/body weight ratio. The decreased body weight in Dox-treated mice may due to the side effects of Dox itself and the decrease in food intake, while the increased lung/body weight ratio may be a result of decreased body weight in these treatment groups. Collectively, these data suggest that decreases in STIM1 and SOCE expression may be associated with the pathogenesis of Dox cardiotoxicity.

Cardiomyocyte apoptosis is one of the major pathogenic mechanisms underlying Dox cardiotoxicity. Accumulating evidence indicates that inhibition of cardiomyocyte apoptosis could effectively minimize myocardial injury, and thus prevent the occurrence of heart failure.[2,3,6] There is a complicated crosstalk between SOCE and cell apoptosis. Several lines of evidence have shown that upregulation of STIM1 and/or ORAI1 promotes sodium butyrate-induced

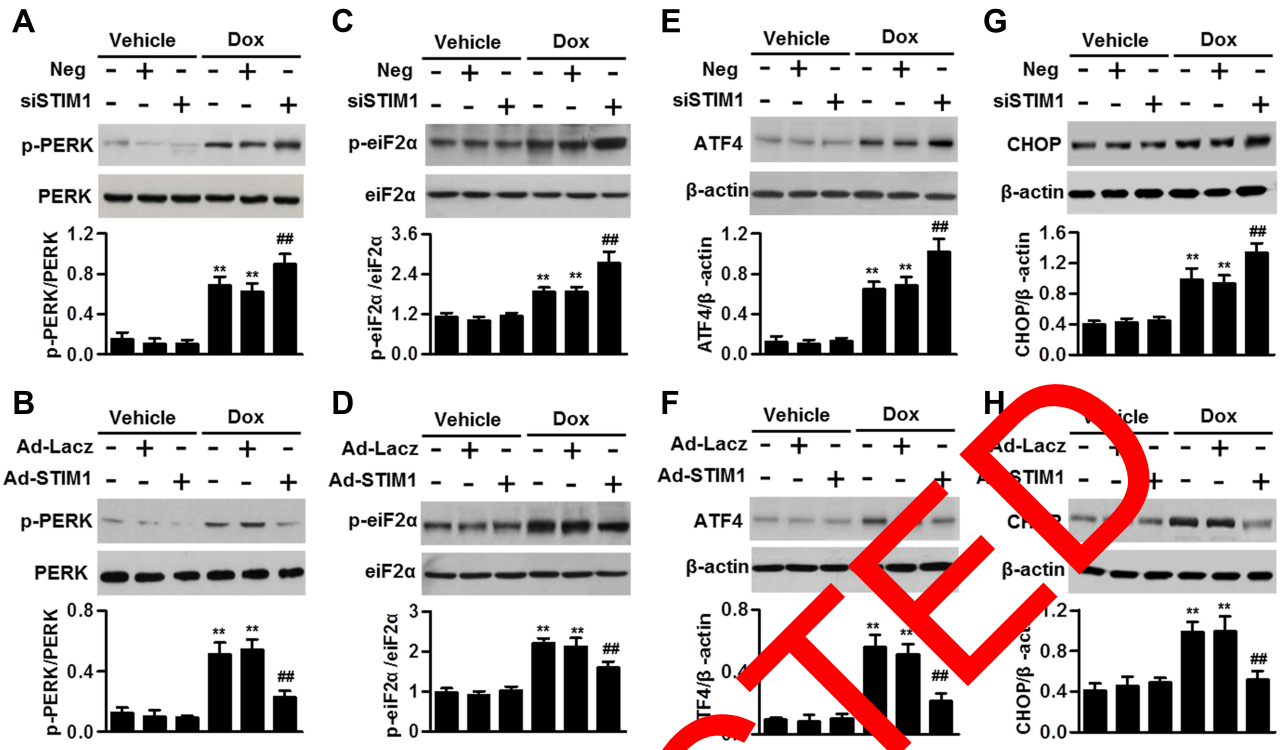

Figure 6 STIM1 downregulation potentiates Dox-induced ER stress. (**A**–**D**) AC16 human cardiomyocytes were transfected with STIM1 siRNA (40 nmol/L) (**A** and **C**), STIM1 adenovirus (40 MOI) (**B** and **D**), or their corresponding negative control, and then incubated with Dox (10 μmol/L) for 1 h. The phosphorylation of PERK (**A** and **B**) and eiF2α (**C** and **D**) were determined. (**E**–**H**) The cells were treated with STIM1 siRNA (**E** and **G**) or STIM1 adenovirus (**F** and **H**) followed by incubation with Dox (10 μmol/L) for 24 h. The protein expression of ATF4 (**E** and **F**) and CHOP (**G** and **H**) were determined. Data were represented as mean ± SEM. **P<0.01 vs vehicle; ##P<0.01 vs Dox, n=6.

nasopharyngeal carcinoma cell apoptosis.[37] Inhibition of SOCE by STIM1 siRNA prevents epithelial cell apoptosis induced by soft substrates.[38] However, other studies have reported that forced SOCE is insufficient to slow down cell death. For example, pharmacological inhibition of SOCE increases the sensitivity of hepatocarcinoma cells to 5-fluorouracil due to induction of autophagic cell death.[39] In addition, STIM1 knockdown enhances non-small cell lung cancer cell apoptosis in response to chemotherapeutic drugs.[40] In this study, cardiomyocyte-specific deficiency of Stim1 significantly promoted myocardial and cardiomyocyte apoptosis upon Dox stimulation as evidenced by TUNEL staining and cytometry using Annexin V/PI staining. The pro-apoptotic effects were associated with down-regulated Bcl-2 expression and the ratio of Bcl-2 to Bax. In contrast, it was reported that suppression of Stim1 inhibited hypoxia/reoxygenation-induced apoptosis in immortalized H9C2 cardiomyocytes.[19] This discrepancy could be due to the different roles of SOCCs in different types of cells, the difference in the change and/or extent of SOCE induced by different stimuli even in the same types of cells, or differing responses of SOCCs in vitro compared to in vivo.

Ca^{2+} is indispensable for the chaperone activity of many ER proteins, and dysfunction of these proteins induces ER stress.[7,12,13] Induction of ER which plays a major role in protein folding and calcium homeostasis has been suggested as a key contributor to cardiac complications of Dox.[11,12] Several UPR signaling sensors have been extensively characterized in ER stress. They include PERK, IRE1α/JNK, ATF6, and caspase 12.[14–16] During ER stress, PERK is autophosphorylated, which promotes eiF2α phosphorylation and downstream ATF4 and CHOP expression.[18] Activated CHOP facilitates the transcription of apoptosis-related genes, resulting in cell apoptosis.[27] IRE1α is another branch of UPR signaling. When ER stress passes a critical threshold, IRE1α can activate JNK-dependent ER stress, driving cells to apoptosis.[14] ATF6 can be translocated into the Golgi apparatus under ER stress conditions, directly regulating the expression of genes encoding ER-associated degradation.[41] In addition, activated caspase 12 is proposed to be another mediator of ER stress-related pro-apoptotic signaling.[42] Consistent with previous studies,[6,30] we confirmed that Dox could significantly induce ER stress, as evidenced by the

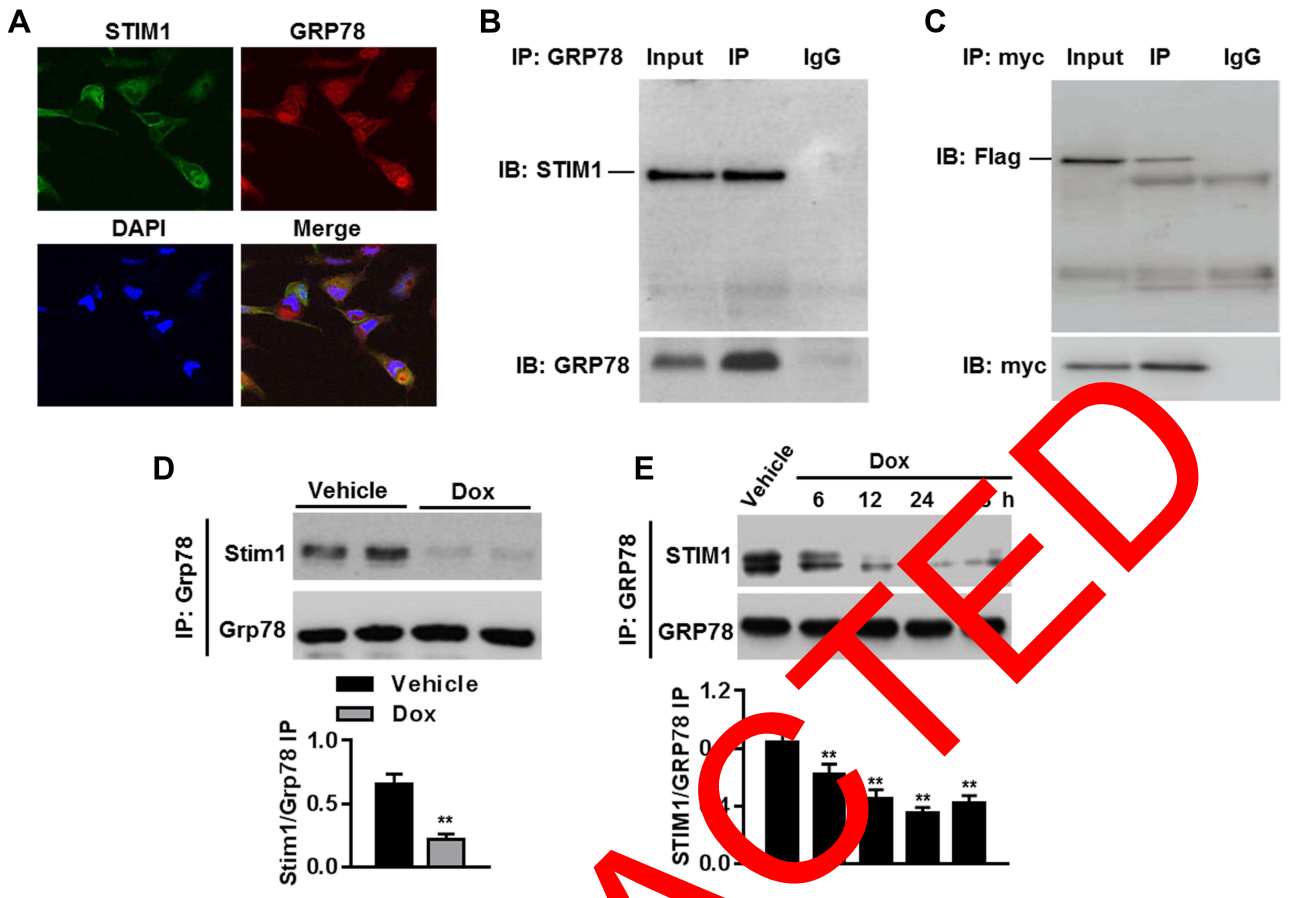

Figure 7 STIM1 relieves ER stress by binding to GRP78 in cardiomyocytes. (**A**) Representative images of STIM1 and GRP78 distribution in cardiomyocytes. (**B**) Cell lysates were immunoprecipitated with anti-GRP78 antibody and immunoprecipitated (IP) proteins were immunoblotted (IB) with anti-STIM1 antibody. n=5. (**C**) Cardiomyocytes were co-transfected with STIM1-flag plasmid and GRP78-myc plasmid. After myc antibody was immunoprecipitated and immunoblotted with anti-flag antibody. n=4. (**D**) Immunoblotting for Stim1 after immunoprecipitation with anti-Grp78 antibody in myocardium from vehicle- or Dox-treated mice. **P<0.01 vs vehicle, n=6/group. (**E**) Cardiomyocytes were treated with Dox (1 μmol/L) for different times. Co-immunoprecipitation analysis was performed to determine the interaction between STIM1 and GRP78. **P<0.01 vs vehicle, n=4.

increased phosphorylation of PERK, eiF2α and JNK and the expression of ATF4, ATF6, and CHOP. The observations that Stim1 overexpression inhibited the phosphorylation of PERK and eiF2α and expression of ATF4 and CHOP strongly suggests that Stim1 attenuates Dox-induced cardiomyocyte apoptosis by inhibiting ER stress-related PERK/eiF2α/ATF4/CHOP UPR signaling. Moreover, it appears that the beneficial effects of Stim1 on UPR induction may bypass the step of JNK/ATF6/caspase 12 because Stim1 did not alter JNK phosphorylation, ATF6 expression, and caspase 12 cleavage. Furthermore, GRP78 is a major ER chaperone protein that initiates the UPR.[17] The present findings show that STIM1 can directly interact with GRP78. The sequestration of GRP78 by STIM1 led to decreased binding of unfolded protein substrates to GRP78, contributing to the acquisition of anti-apoptotic capacity. Collectively, these data indicate that stabilizing Stim1 in cardiomyocytes may be necessary for the inhibition of ER stress and cardiomyocyte apoptosis.

There are some limitations in the present study. Firstly, although the effect of Dox on Stim1 expression is suggested to be associated with post-translational regulation, further detailed mechanism by which Dox induces Stim1 protein expression downregulation remains to be explored. Secondly, we did not set a positive control throughout the study. Thirdly, we used AC16 cells in the study of mechanism, although the in vivo data demonstrated that cardiomyocyte-specific deficiency of Stim1 exacerbated Dox cardiotoxicity. The AC16 cells may not fully represent primary cardiomyocytes. Thus, further research is indispensable to better understand the specific role of Stim1 in Dox cardiotoxicity and the related mechanisms.

These findings provide the first evidence of the anti-apoptotic property of STIM1 in cardiomyocytes, which is mediated by GRP78-dependent ER stress. Additionally, this study offers a rational therapeutic strategy to protect against Dox cardiotoxicity.

Abbreviations

Dox, doxorubicin; Ca^{2+}, calcium ion; SOCE, store-operated Ca^{2+} entry; SOCCs, store-operated Ca^{2+} channels; ER, endoplasmic reticulum; UPR, unfolded protein response; PERK, PKR-like ER kinase; eiF2α, eukaryotic translation initiation factor-α; CHOP, C/EBP-homologous protein; IRE1α, inositol-requiring enzyme 1α; Ad, adenovirus; AAV, adeno-associated virus; $[Ca^{2+}]_i$, intracellular Ca^{2+} concentration; LVPWth, left ventricular end-diastolic posterior wall thickness; LVDd, left ventricular end-diastolic diameter; LVDs, left ventricular end-systolic diameter; EF, ejection fraction; FS, fractional shortening; LDH, lactate dehydrogenase; cTnT, cardiac troponin T.

Author Contributions

All authors made a significant contribution to the work reported, whether that is in the conception, study design, execution, acquisition of data, analysis and interpretation, or in all these areas; took part in drafting, revising or critically reviewing the article; gave final approval of the version to be published; have agreed on the journal to which the article has been submitted, and agree to be accountable for all aspects of the work.

Funding

This work was supported by Basic Research of Medical Science of Suzhou (SYS2019074), Young Medical Talents of Jiangsu Province (QNRC2016876), Health Talents Training Project of Gusu District (GSWS2019040), Research Foundation from the Second Affiliated Hospital of Soochow University (XKTJ-TD202008), and the Special Fund for the Cultivation of High-level Health Technical Personnel in Yunnan Province (D-2018050).

Disclosure

The authors declare that they have no competing interests.

References

1. Yeh ET, Tong AT, Lenihan DJ, et al. Cardiovascular complications of cancer therapy: diagnosis, pathogenesis, and management. *Circulation*. 2004;109(25):3122–3131. doi:10.1161/01.CIR.0000133187.74800.B9
2. Jing X, Yang J, Jiang L, Chen J, Wang H. MicroRNA-29b regulates the mitochondria-dependent apoptotic pathway by targeting Bax in doxorubicin cardiotoxicity. *Cell Physiol Biochem*. 2018;48(2):692–704. doi:10.1159/000491896
3. Zhang S, Liu X, Bawa-Khalfe T, et al. Identification of the molecular basis of doxorubicin-induced cardiotoxicity. *Nat Med*. 2012;18(11):1639–1642. doi:10.1038/nm.2919
4. Fujisaki G, Inokuchi C, Murashige N. Doxorubicin-induced myocardial injury. *N Engl J Med*. 2004;351(18):1908–1909;author reply 1908–1909.
5. Zagar TM, Cardinale DM, Marks LB. Breast cancer therapy-associated cardiovascular disease. *Nat Rev Clin Oncol*. 2016;13(3):172–184. doi:10.1038/nrclinonc.2015.171
6. Chen R, Sun G, Yang L, Wang J, Sun X. Salvianolic acid B protects against doxorubicin induced cardiac dysfunction via inhibition of ER stress mediated cardiomyocyte apoptosis. *Toxicol Res (Camb)*. 2016;5(5):1335–1345. doi:10.1039/C6TX00111D
7. Schroder M, Kaufman RJ. ER stress and the unfolded protein response. *Mutat Res*. 2005;569(1–2):29–63.
8. Ren J, Bi Y, Sowers JR, Hetz C, Zhang Y. Endoplasmic reticulum stress and unfolded protein response in cardiovascular diseases. *Nat Rev Cardiol*. 2021;18(7):499–521.
9. Walter P, Ron D. The unfolded protein response: from stress pathway to homeostatic regulation. *Science*. 2011;334(6059):1081–1086. doi:10.1126/science.1209038
10. Chang WT, Li YW, Ho CH, Chen ZC, Liu PY, Shih JY. Dapagliflozin suppresses ER stress and protects doxorubicin-induced cardiotoxicity in breast cancer patients. *Arch Toxicol*. 2021;95(2):659–671. doi:10.1007/s00204-020-02951-8
11. Yarmohammadi F, Rezaee R, Haye AW, Karimi G. Endoplasmic reticulum stress in doxorubicin-induced cardiotoxicity may be therapeutically targeted by natural and chemical compounds: a review. *Pharmacol Res*. 2021;164:105383. doi:10.1016/j.phrs.2020.105383
12. Zhou H, Wang J, Zhu P, Hu S, Ren J. Ripk3 regulates cardiac microvascular reperfusion injury: the role of IP3R-dependent calcium overload, XO-mediated oxidative stress and F-action/filopodia-based cellular migration. *Cell Signal*. 2018;45:12–22. doi:10.1016/j.cellsig.2018.01.020
13. Sun X, Wei Q, Cheng J, et al. Enhanced Stim1 expression is associated with acquired chemo-resistance of cisplatin in osteosarcoma cells. *Hum Cell*. 2017;30(3):216–225. doi:10.1007/s13577-017-0167-9
14. Chen Y, Brandizzi F. IRE1: ER stress sensor and cell fate executor. *Trends Cell Biol*. 2013;23(11):547–555. doi:10.1016/j.tcb.2013.06.005
15. Gardner BM, Pincus D, Gotthardt K, Gallagher CM, Walter P. Endoplasmic reticulum stress sensing in the unfolded protein response. *Cold Spring Harb Perspect Biol*. 2013;5(3):a013169. doi:10.1101/cshperspect.a013169
16. Kaneko M, Imaizumi K, Saito A, et al. ER stress and disease: toward prevention and treatment. *Biol Pharm Bull*. 2017;40(9):1337–1343. doi:10.1248/bpb.b17-00342
17. Okada T, Yoshida H, Akazawa R, Negishi M, Mori K. Distinct roles of activating transcription factor 6 (ATF6) and double-stranded RNA-activated protein kinase-like endoplasmic reticulum kinase (PERK) in transcription during the mammalian unfolded protein response. *Biochem J*. 2002;366(Pt 2):585–594. doi:10.1042/bj20020391
18. Ma Y, Hendershot LM. The unfolding tale of the unfolded protein response. *Cell*. 2001;107(7):827–830. doi:10.1016/S0092-8674(01)00623-7
19. He F, Wu Q, Xu B, et al. Suppression of Stim1 reduced intracellular calcium concentration and attenuated hypoxia/reoxygenation induced apoptosis in H9C2 cells. *Biosci Rep*. 2017;37(6). doi:10.1042/BSR20171249
20. Pang Y, Hunton DL, Bounelis P, Marchase RB. Hyperglycemia inhibits capacitative calcium entry and hypertrophy in neonatal cardiomyocytes. *Diabetes*. 2002;51(12):3461–3467. doi:10.2337/diabetes.51.12.3461

21. Collins HE, Zhu-Mauldin X, Marchase RB, Chatham JC. STIM1/Orai1-mediated SOCE: current perspectives and potential roles in cardiac function and pathology. *Am J Physiol Heart Circ Physiol*. 2013;305(4):H446–458. doi:10.1152/ajpheart.00104.2013
22. Vig M, Peinelt C, Beck A, et al. CRACM1 is a plasma membrane protein essential for store-operated Ca2+ entry. *Science*. 2006;312(5777):1220–1223. doi:10.1126/science.1127883
23. Yeromin AV, Zhang SL, Jiang W, Yu Y, Safrina O, Cahalan MD. Molecular identification of the CRAC channel by altered ion selectivity in a mutant of Orai. *Nature*. 2006;443(7108):226–229. doi:10.1038/nature05108
24. Luo X, Hojayev B, Jiang N, et al. STIM1-dependent store-operated Ca(2)(+) entry is required for pathological cardiac hypertrophy. *J Mol Cell Cardiol*. 2012;52(1):136–147. doi:10.1016/j.yjmcc.2011.11.003
25. Liang SJ, Zeng DY, Mai XY, et al. Inhibition of Orai1 store-operated calcium channel prevents foam cell formation and atherosclerosis. *Arterioscler Thromb Vasc Biol*. 2016;36(4):618–628. doi:10.1161/ATVBAHA.116.307344
26. Pachon RE, Scharf BA, Vatner DE, Vatner SF. Best anesthetics for assessing left ventricular systolic function by echocardiography in mice. *Am J Physiol Heart Circ Physiol*. 2015;308(12):H1525–1529. doi:10.1152/ajpheart.00890.2014
27. Wali JA, Rondas D, McKenzie MD, et al. The proapoptotic BH3-only proteins Bim and Puma are downstream of endoplasmic reticulum and mitochondrial oxidative stress in pancreatic islets in response to glucotoxicity. *Cell Death Dis*. 2014;5:e1124. doi:10.1038/cddis.2014.88
28. Glab JA, Cao Z, Puthalakath H. Bcl-2 family proteins, beyond the veil. *Int Rev Cell Mol Biol*. 2020;351:1–22.
29. Liu XY, Zhang FR, Shang JY, et al. Renal inhibition of miR-181a ameliorates 5-fluorouracil-induced mesangial cell apoptosis and nephrotoxicity. *Cell Death Dis*. 2018;9(6):610. doi:10.1038/s4141[illegible]018-0677-8
30. Hu J, Wu Q, Wang Z, et al. Inhibition of CACNA1[illegible]ttenuates doxorubicin-induced acute cardiotoxicity by affecting endo[illegible]smic reticulum stress. *Biomed Pharmacother*. [illegible]019;120:[illegible]9475. doi:10.1016/j.biopha.2019.109475
31. Wang Z, Wang M, Liu J, et al. Inhibiti[illegible] of T[illegible]A attenuates doxorubicin-induced acute cardiotoxici[illegible]by suppress[illegible] oxidative stress, the inflammatory response, an[illegible]lasmic reticu[illegible] stress. *Oxid Med Cell Longev*. 2018;2[illegible]18:5179[illegible] doi:10.1155/2018/5179468
32. Kojima A, Kitagawa H, Omatsu-Kanbe M, Matsuura H, Nosaka S. Ca2+ paradox injury mediated through TRPC channels in mouse ventricular myocytes. *Br J Pharmacol*. 2010;161(8):1734–1750. doi:10.1111/j.1476-5381.2010.00986.x
33. Benard L, Oh JG, Cacheux M, et al. Cardiac Stim1 silencing impairs adaptive hypertrophy and promotes heart failure through inactivation of mTORC2/Akt signaling. *Circulation*. 2016;133(15):1458–1471; discussion 1471. doi:10.1161/CIRCULATIONAHA.115.020678
34. Liu X, Chang Y, Choi SY, Pan Z. Blocking store-operated Ca2+ entry to protect cardiomyocytes from epirubicin-induced toxicity. *FASEB J*. 2020;34(S1):1. doi:10.1096/fasebj.2020.34.s1.06876
35. Arafa MH, Mohammad NS, Atteia HH, Abd-Elaziz HR. Protective effect of resveratrol against doxorubicin-induced cardiac toxicity and fibrosis in male experimental rats. *J Physiol Biochem*. 2014;70(3):701–711. doi:10.1007/s13105-014-0339-[illegible]
36. Shoukry HS, Ammar HI, Rashed LA, et[illegible] Prophy[illegible]tic supplementation of resveratrol is more effective[illegible]an its therapeu[illegible] use against doxorubicin induced cardiotoxicity. *PL[illegible]One*. 2017;12[illegible]:e0181535. doi:10.1371/journal.pone.01815[illegible]
37. Huang W, Ren C, Huang G[illegible]al. Inhibition[illegible]store-[illegible]erated Ca(2+) entry counteracts the ap[illegible]tosis of [illegible]opharyn[illegible]carcinoma cells induced by sodium b[illegible]rate. [illegible]col Lett*. 2017;13(2):921–929. doi:10.3892/ol.201[illegible]469
38. Chiu WT, Tang[illegible]J, Jao HC, [illegible]en MR[illegible]oft substrate up-regulates the interactio[illegible]STIM1 with stor[illegible]ated Ca2+ channels that lead to normal epithel[illegible] cell apoptosis. *Mol Biol Cell*. 2008;19(5):2220–2230. doi:10.[illegible]91/mbc.e07-11-1170
39. Tan[illegible]BD, Xia X, Lv XF, [illegible]l. Inhibition of Orai1-mediated Ca(2+) entry enhances chemosensitivity of HepG2 hepatocarcinoma cells to 5-fluorouracil. *J[illegible]ell Mol Med*. 2017;21(5):904–915. doi:10.1111/j[illegible]m.13029
40. Li[illegible] Zhang M[illegible] Xu L, Lin D, Cai S, Zou F. The apoptosis of non-sm[illegible]ung cancer induced by cisplatin through modulation [illegible]f STIM1. *Exp Toxicol Pathol*. 2013;65(7–8):1073–1081. doi:[illegible]016/j.etp.2013.04.003
41. Lee K, Tirasophon W, Shen X, et al. IRE1-mediated unconventional mRNA splicing and S2P-mediated ATF6 cleavage merge to regulate XBP1 in signaling the unfolded protein response. *Genes Dev*. 2002;16(4):452–466. doi:10.1101/gad.964702
42. van der Kallen CJ, van Greevenbroek MM, Stehouwer CD, Schalkwijk CG. Endoplasmic reticulum stress-induced apoptosis in the development of diabetes: is there a role for adipose tissue and liver? *Apoptosis*. 2009;14(12):1424–1434. doi:10.1007/s10495-009-0400-4